Neutron scattering for *in-situ* characterization of Li-ion batteries (LIB)

Anatoly M. Balagurov, bala@nf.jinr.ru

L. F. Nazar (Canada) "The role of neutron diffraction in understanding energy storage materials" ICNS, 2013

- **LIBs: the most effective energy storage**
- **NS for electrochemistry**
- **NS for LIBs**
- **FLNP, Dubna: current work**

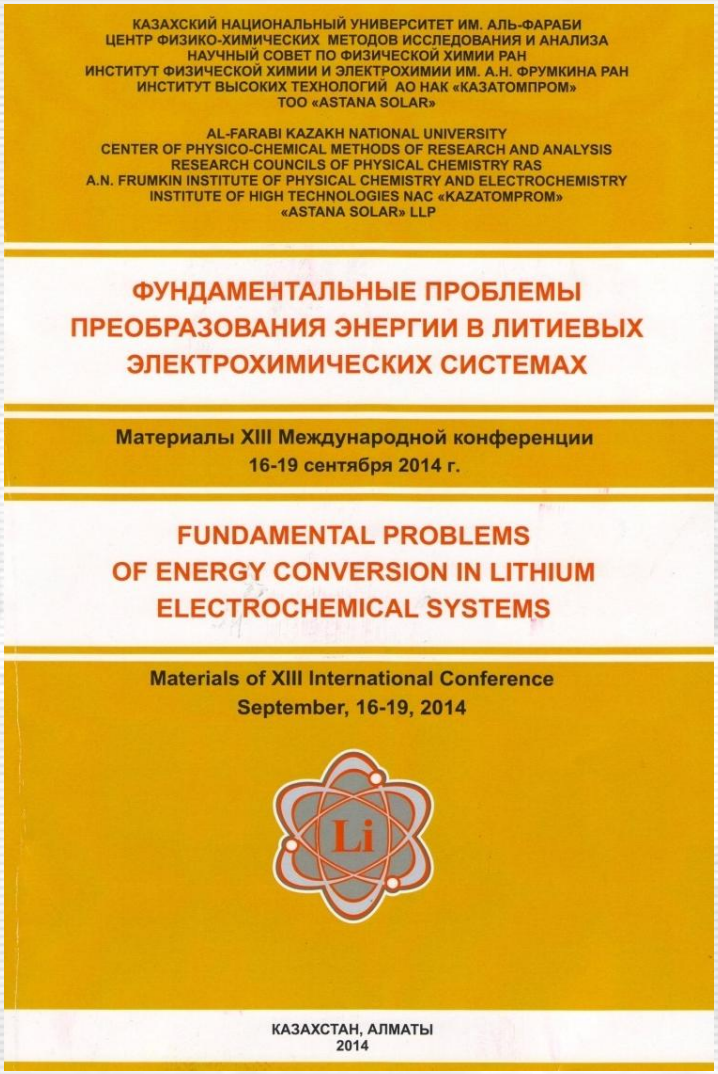

ОАО "Сатурн" Краснодар

Ракетно-космический центр "Прогресс" Самара

ООО "Завод электрохимических преобразователей" Новоуральск

ЗАО "Орион-ХИТ", Новочеркасск

Электрохимические источники энергии

Топливный элемент (Fuel Cell) - электрохимическое устройство, преобразующее энергию химической реакции в электрическую энергию при использованию подающихся извне топлива и окислителя (открытая система).

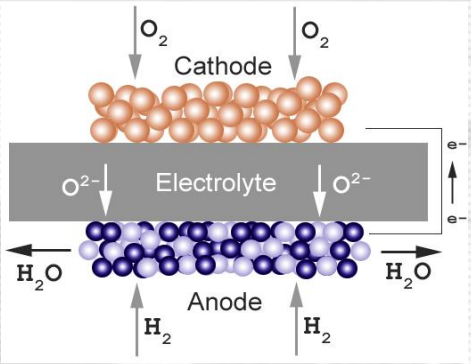

катод: $\frac{1}{2} O_2 + 2e^- \rightarrow O^{2-}$

анод: $O^{2-} + H_2 \rightarrow H_2O + 2e^-$

электролит - Y_2O_3/ZrO_2
анод - $CoZrO_2$
катод - $La(Sr)MnO_3$

SOFC: Твердооксидная топливная ячейка. Рабочая температура: 600-1000 C

Батареи и аккумуляторы - электрохимическое устройство, в котором электроэнергия генерируется при преобразовании химической энергии с помощью обратимых *redox* реакций на электродах (закрытые системы с одновременным хранением и преобразованием энергии).

Redox = reduction / oxidation = gain / loss of electrons

Литий-ионный аккумулятор

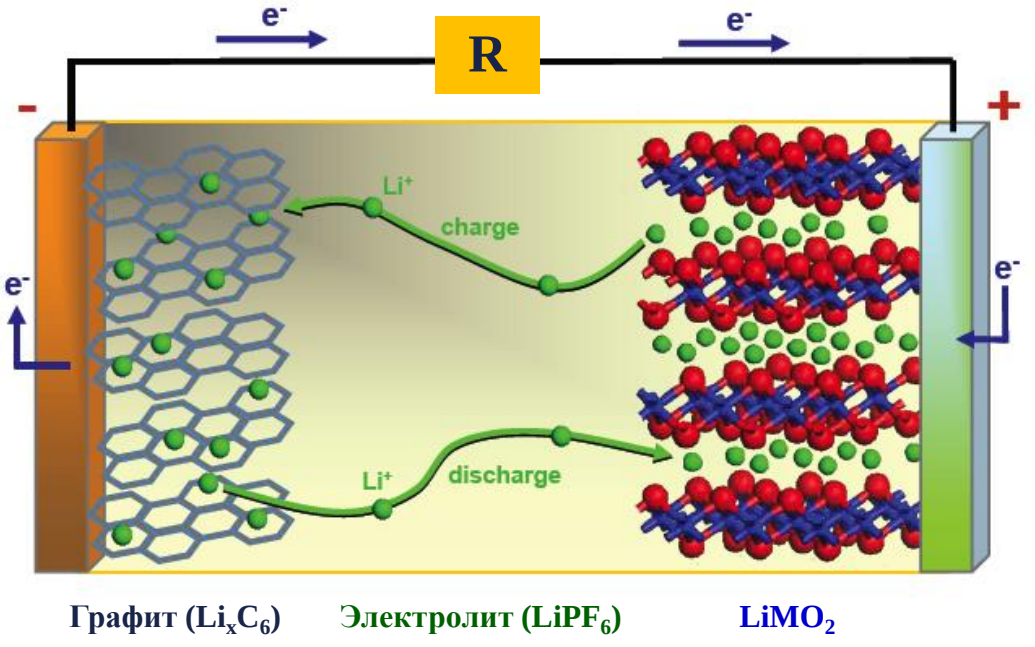

Графит (Li_xC_6) Электролит ($LiPF_6$) $LiMO_2$

John B. Goodenough
USA, 1922

K.Mizushima, P.Jones, P.Wiseman, J.B.Goodenough "Li_xCoO_2 (0<x<-1): A new cathode material for batteries of high energy density", 1980) 783–789

$$C_6 + LiCoO_2 \underset{\text{разряд}}{\overset{\text{заряд}}{\rightleftharpoons}} Li_xC_6 + Li_{1-x}CoO_2$$

$x \approx 0.5\text{-}0.6$

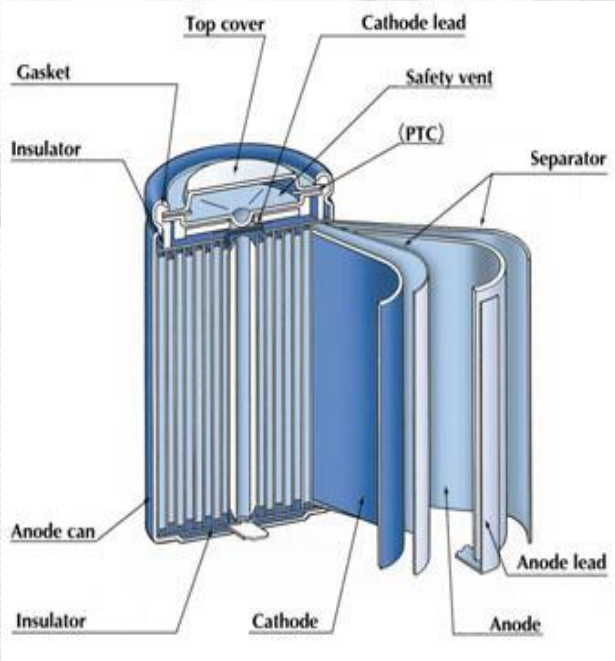

Через 15 – 20 лет автомобили будут электрическими. В качестве источника тока будут использоваться Li-аккумуляторы.

Nissan Leaf NP300

(электромобиль концерна Nissan, серийно выпускается с весны 2010 года)

Total weight	**1521 kg**
Li-ion battery weight	**300 kg**
Stored energy	**24 kWh**
Power	**120 h.p.**
Distance	**~200 km**
Maximum speed	**150 km/h**
Charging time	**8 h (220 V, 8 h)**
Life time	**5 years**
Cathode material	**$LiMn_2O_4$**
Price	**~600,000 rub**

Классный автомобиль владел полгода, для себя увидел только плюсы, электромобиль это будущее!!! Никакого масла, свечей, ремней, топливной системы, бензо-заправок!

Литий-ионный аккумулятор

Энергоемкость (U•I•t)

удельная энергия (Вт·ч/кг)

объемная энергия (Вт·ч/л)

Емкость (А·ч/г)

Рабочее напряжение (В)

Мощность (Вт) **(коэфф. диффузии Li)**

Циклируемость **(деградация электродов)**

Рабочий интервал температур

Время заряда

Безопасность

Стоимость

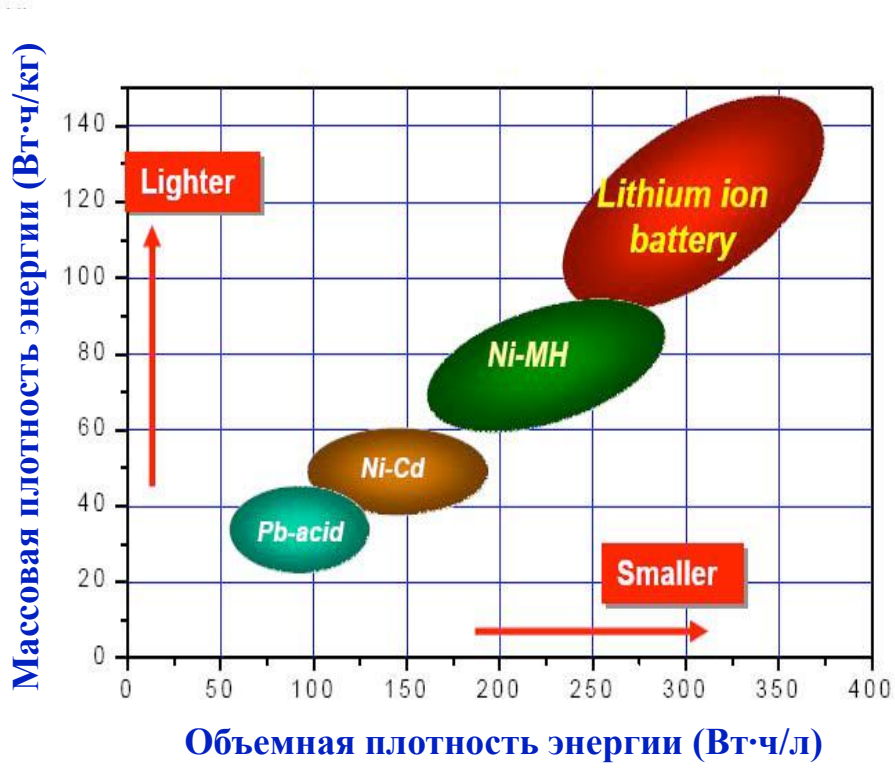

Запасенный заряд

$$\text{Емкость (А·ч/г)} = C_T \sim n/M \sim 0.2\ \text{А·ч/г}$$

Молекулярный вес

Основные материалы для катода

$LiCoO_2$

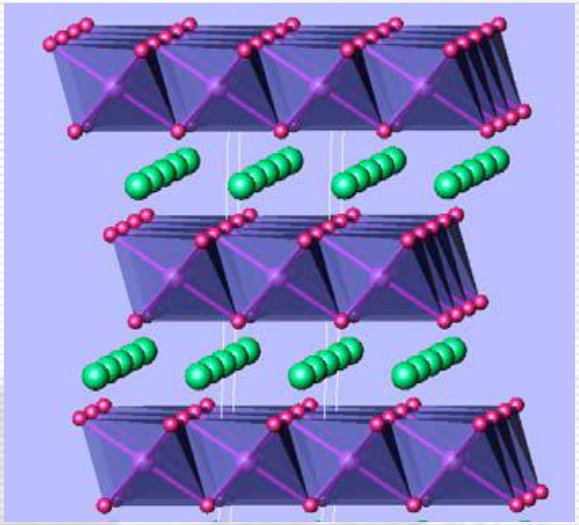

R-3m, *a*=2.8, *c*=14.0 Å

$C_т$ = 278 мА·ч/г

$D = 10^{-9}$ см^2/с

$LiMn_{1/3}Ni_{1/3}Co_{1/3}O_2$

$Li_{1.2}Mn_{0.4}Ni_{0.3}Co_{0.1}O_2$

$LiMn_2O_4$ (шпинель)

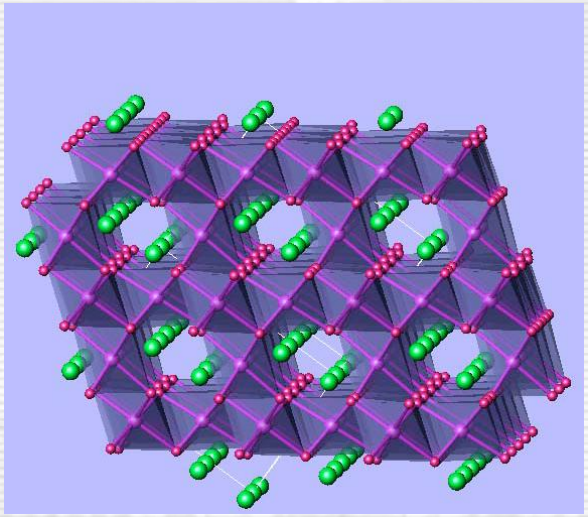

Fd3m, *a* = 8.25 Å

$C_т$ = 148 мА·ч/г

$D = 10^{-10}$ см^2/с

$LiMn_{1.5-x}Ni_{0.5-y}M_{x+y}O_{4-z}$

M = Mg, Al, Co, Cr, Ti

$LiFePO_4$ (оливин)

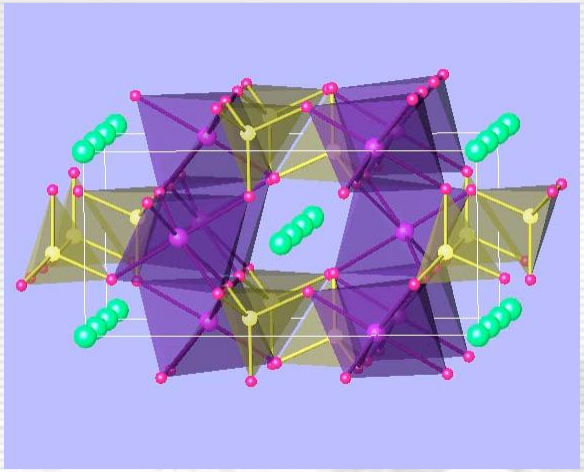

Pnma, *a*=10.3, *b*=6.0, *c*=4.7 Å

$C_т$ = 170 мА·ч/г

$D = 10^{-15}$ см^2/с

$Li_2Co_{1-x}M_xPO_4F$

M = Fe, Mn

Neutron scattering and electrochemistry

1) **Good visibility of light elements and neighboring atoms**
2) **Strong magnetic scattering (magnetic structure)**
3) **Small absorption (high penetration depth)**

Problems, which can be solved with neutron scattering:

- **atomic and magnetic structures of new materials (*ex situ*)**
- **phase transitions in electrode materials (*in situ*)**
- **structural changes in electrodes in the course of redox-processes (*in situ*)**
- **structural processes in electrodes in real units (*in situ*)**
- **defect microstructure of electrodes**
- **…**

- Experiments can be performed in the model conditions using special electrochemical cells and with real batteries;

- All studies can be performed in very large temperature range: 4 – 1300 K.

In situ neutron measurement techniques for LIBs studies

I. Continuous neutron sources

ILL (France)
ANSTO (Australia)
SINQ (Switzerland)
FRM II (Germany)
HANARO (Korea)
NIST (USA)

II. Pulsed neutron sources

LANSCE (USA)
SNS (USA)
IBR-2 (Russia)

Diffraction: atomic, magnetic and defect structures, micro-scale (~0.01 nm)

Reflectometry: multilayer composition, surface structure, meso-scale (~1 nm)

Small angle scattering: non-uniformity of materials, meso-scale (~10 nm)

Imaging: spatial distribution of migrated atoms, macro-scale (~10 μm)

All together, they provide multi-scale view of redox processes in LIBs

Геометрия нейтронного дифракционного эксперимента

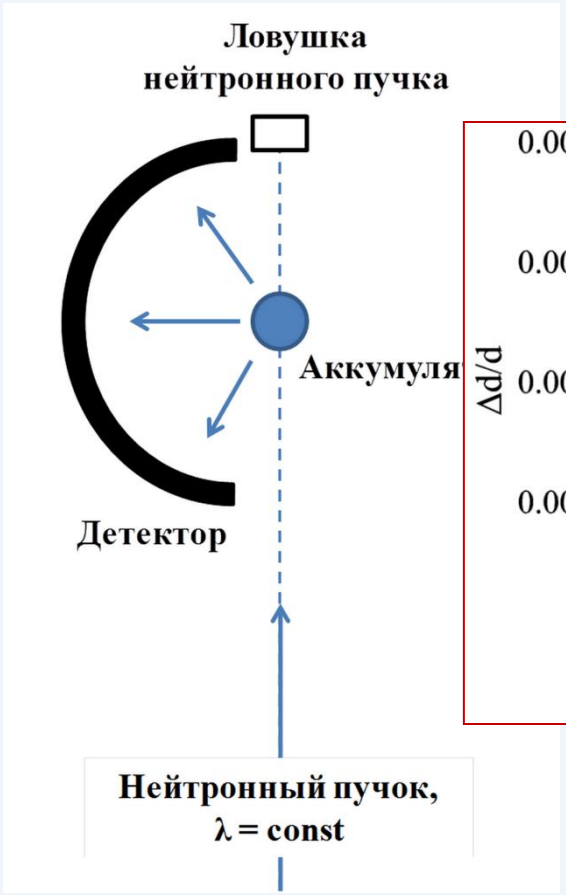

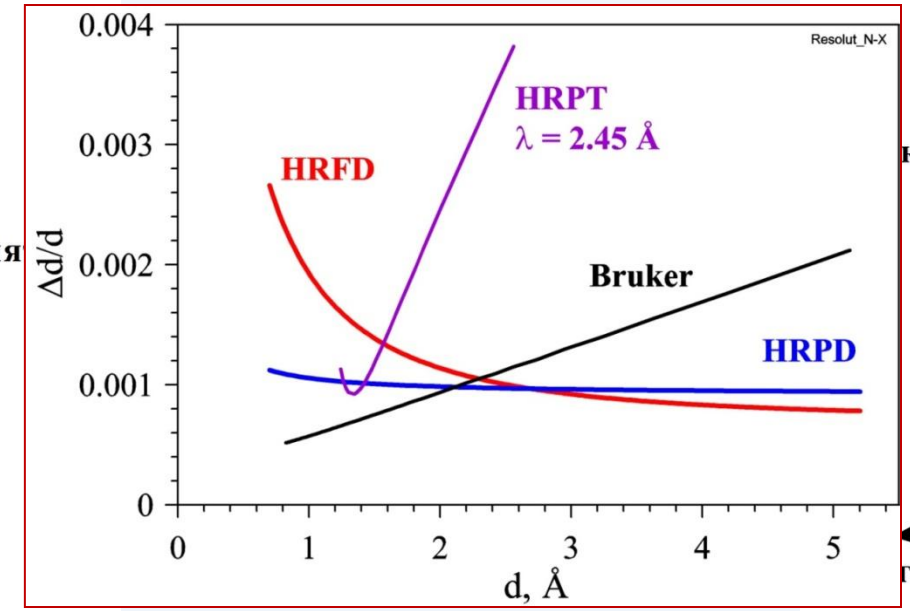

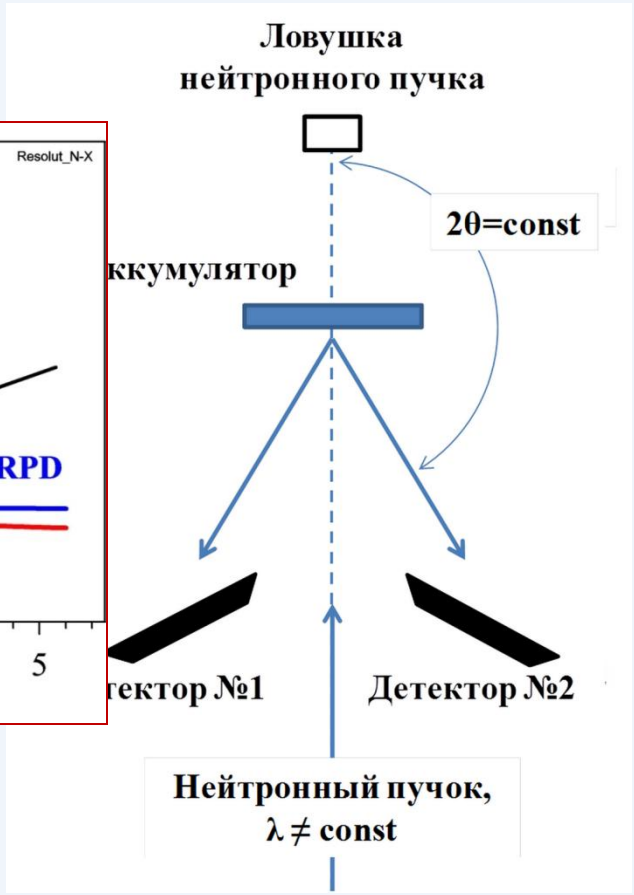

Стационарный источник.

Сканирование по углу рассеяния

Импульсный источник.

Сканирование по длине волны

NAC-стандарт ($Na_2Al_2Ca_3F_{14}$) на TOF- и λ_0 -дифрактометрах

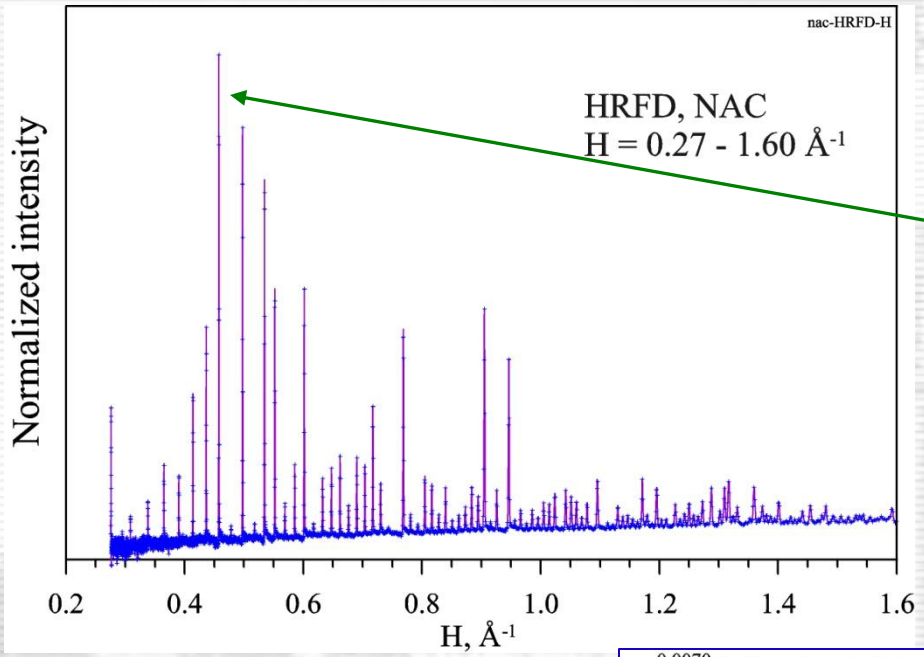

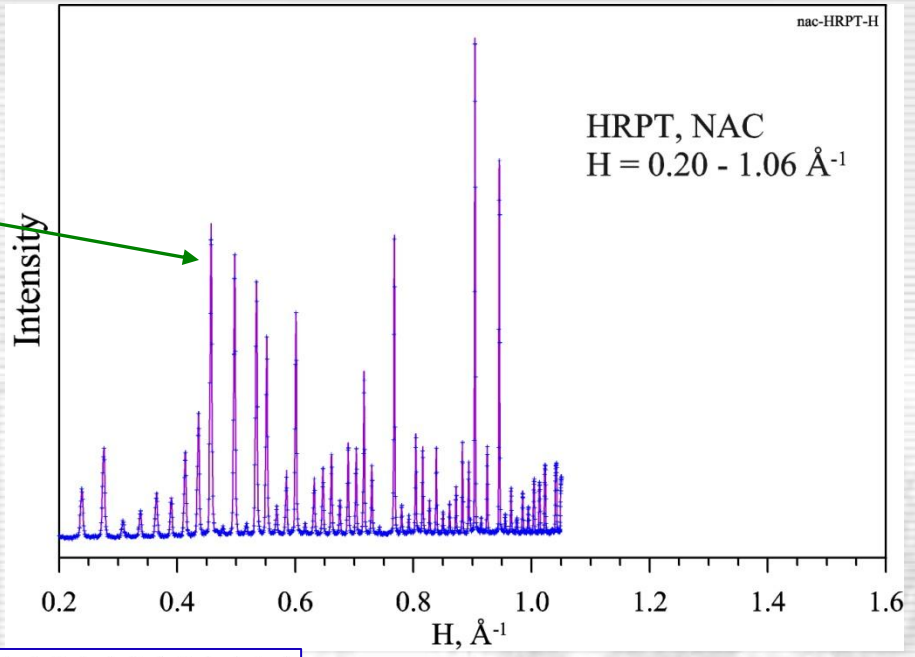

TOF-diffractometer HRFD … meter HRPT: λ_0 = 1.886 Å,

wavelength range = 1.2 – 7. … ngles range = 10 - 165°

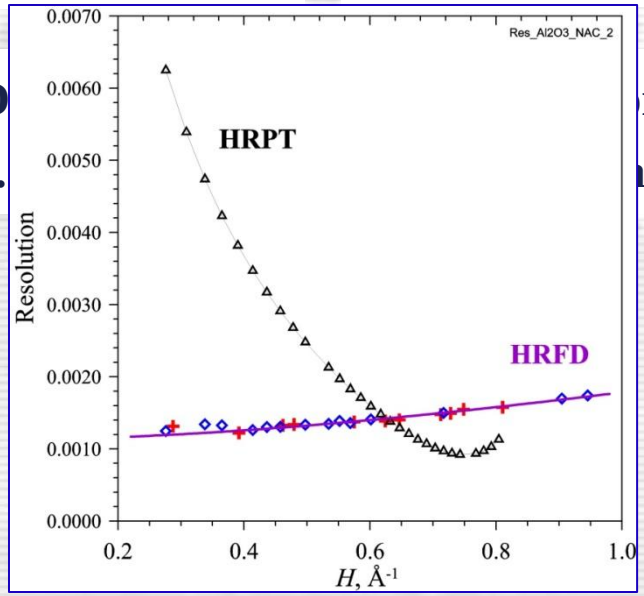

Light atoms and cations distribution in electrode materials

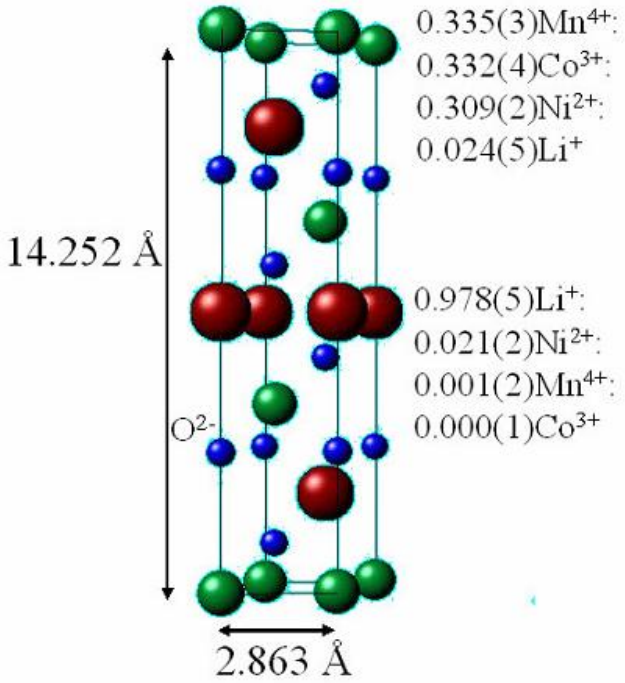

$LiMn_{1/3}Ni_{1/3}Co_{1/3}O_2$ (R-3m)

Joint synchrotron and neutron refinement. About 2% Ni displaced Li from the (3a) site.

97% Li, 3% Ni

11% Mn, 24% Ni, 10% Co, 55% Li

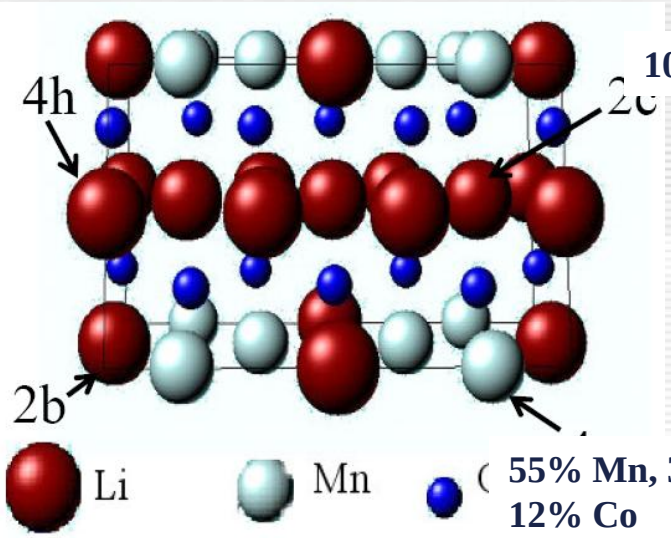

100% Li

55% Mn, 33% Ni, 12% Co

$Li_{1.2}Mn_{0.4}Ni_{0.3}Co_{0.1}O_2$

Crystal structure of Li_2MnO_3 type, C2/m,

a = 4.982, b = 8.562, c = 5.013 Å, β = 109.24

from P.S. Whitfield et al., "Untangling cation ordering in complex lithium battery cathode materials – simultaneous refinement of x-ray, neutron and resonant scattering data" Advances in X-ray Analysis Vol. 49, 2005

Electrochemical cells for *in-situ* neutron diffraction

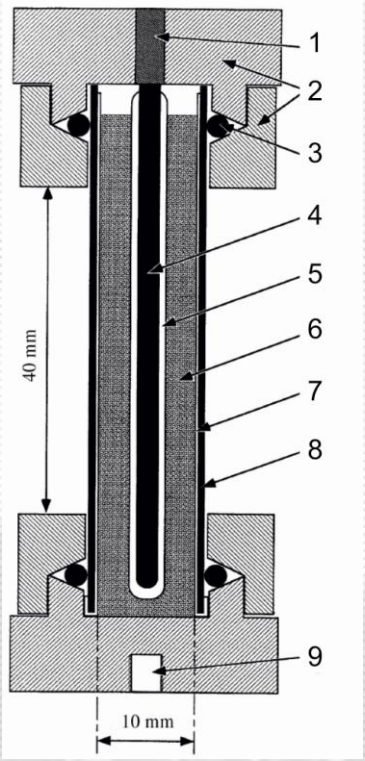

Ö. Bergström et al., 1998

1. контакт для Li анода,
4. Li анод,
5. электролит и сепаратор,
6. электродный материал,
7. 100 нм слой токосъемника,
8. трубка Pyrex®,
9. держатель.

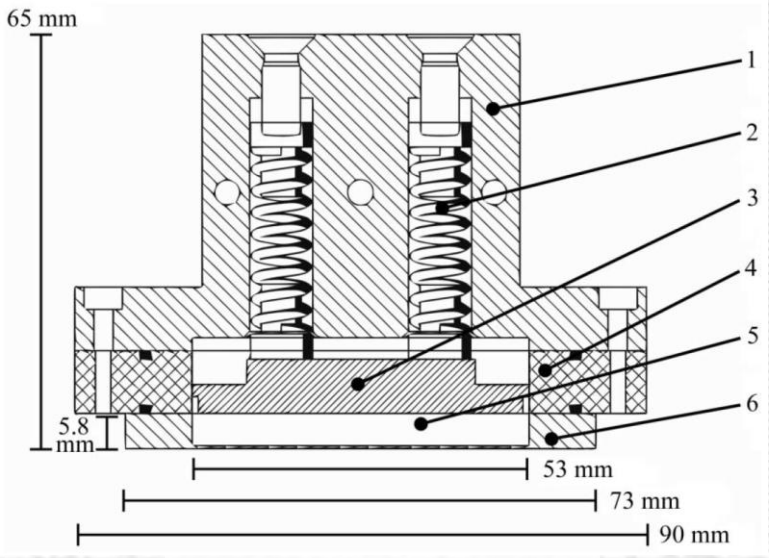

F.Rosciano et al., 2008

1. крышка ячейки,
2. пружины и клапаны,
3. медный токосъемник,
4. корпус ячейки,
5. отсек для рабочего электрода,
6. алюминиевый токосъемник.

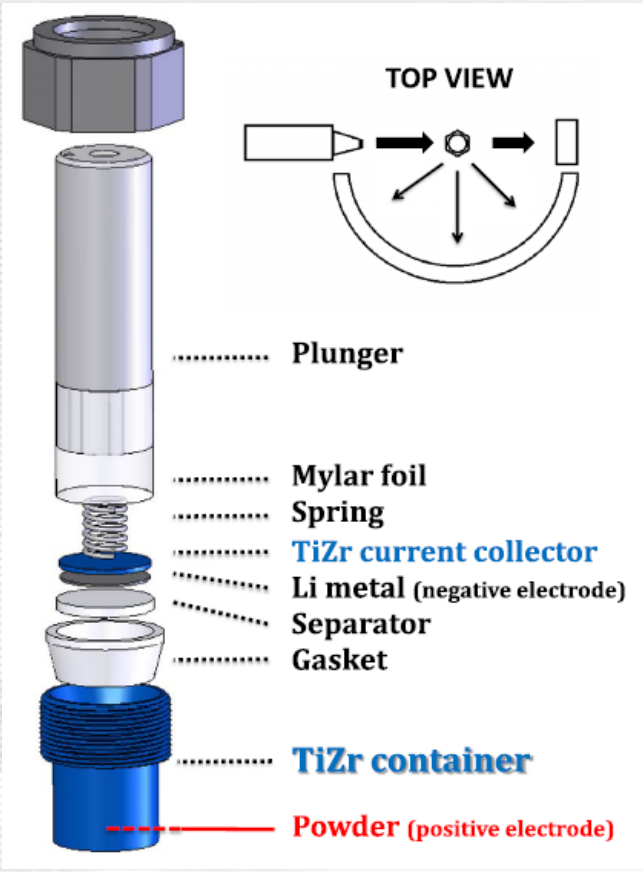

J.Bianchini et al., 2013

ILL, D20, λ = 1.547 Å
m = 10 – 200 mg,
t_s = 10 - 30 min

In-operando neutron diffraction at D20 (ILL): $LiFePO_4 \rightarrow FePO_4$

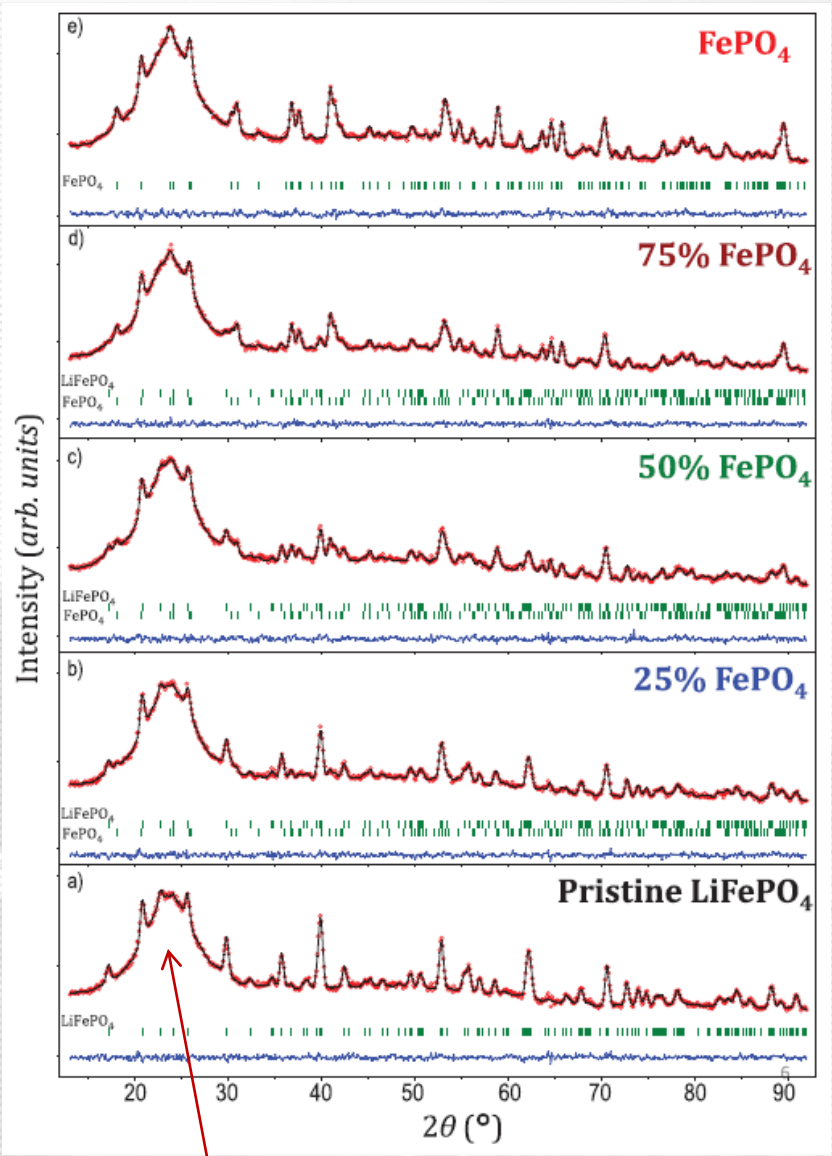

Electrolyte: ($LiPF_6$ + d-Ethylene Carbonate)

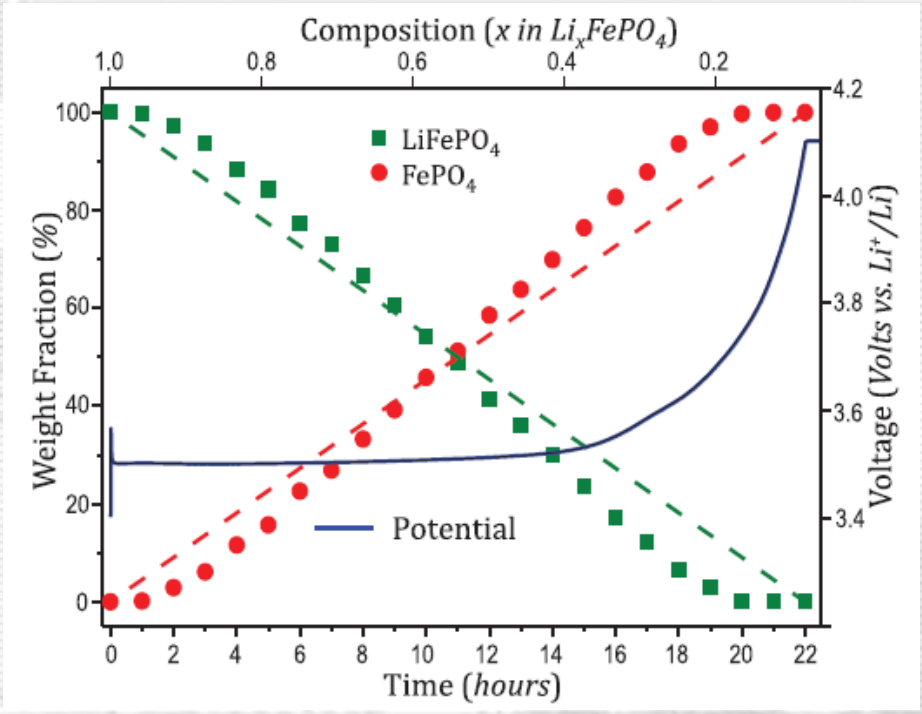

Weight fractions for $LiFePO_4$ and $FePO_4$, determined from neutron diffraction data recorded operando during Li^+ extraction from $LiFePO_4$.

ILL, D20, λ = 1.547 Å
m = 200 mg, t_s = 60 min

J.Bianchini et al., 2013

In Situ Neutron diffraction study of the a commercial (CLEON Technologies Sdn Bhd) Li-ion cell, Wombat, ANSTO, Australia

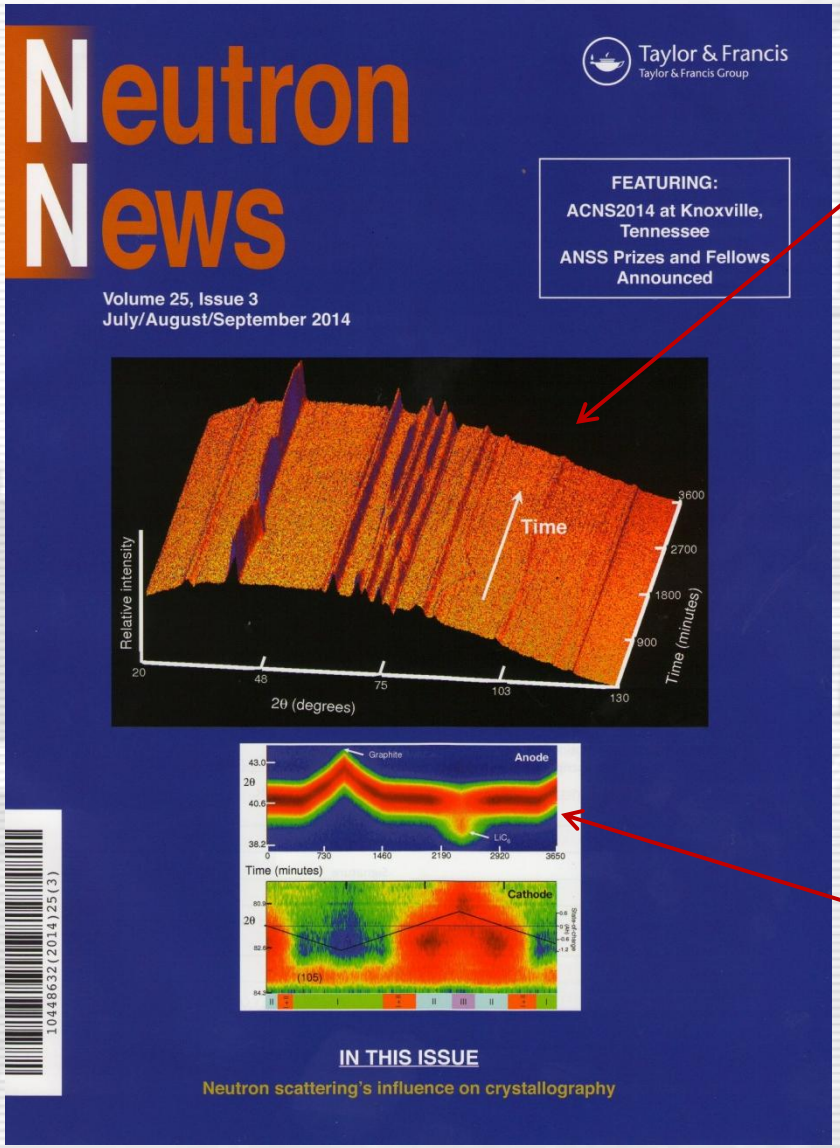

ND patterns collected as a function of time during electrochemical cycling. Cell is discharged to 3.2 V, followed by charging to 4.2 V and final discharge.

Materials:

- **$LiCoO_2$ type cathode**
- **graphite (Li_xC_6) anode**
- **Al current collector**
- **electrolyte (background)**

ND patterns of graphite and LiC_n reflections. Splitting and formation of stoichiometric LiC_6 is shown near charged state of battery.

from Neeraj Sharma et al., J. Power Sources 195 (2010) 8258

In Situ ND at the IBR-2 reactor

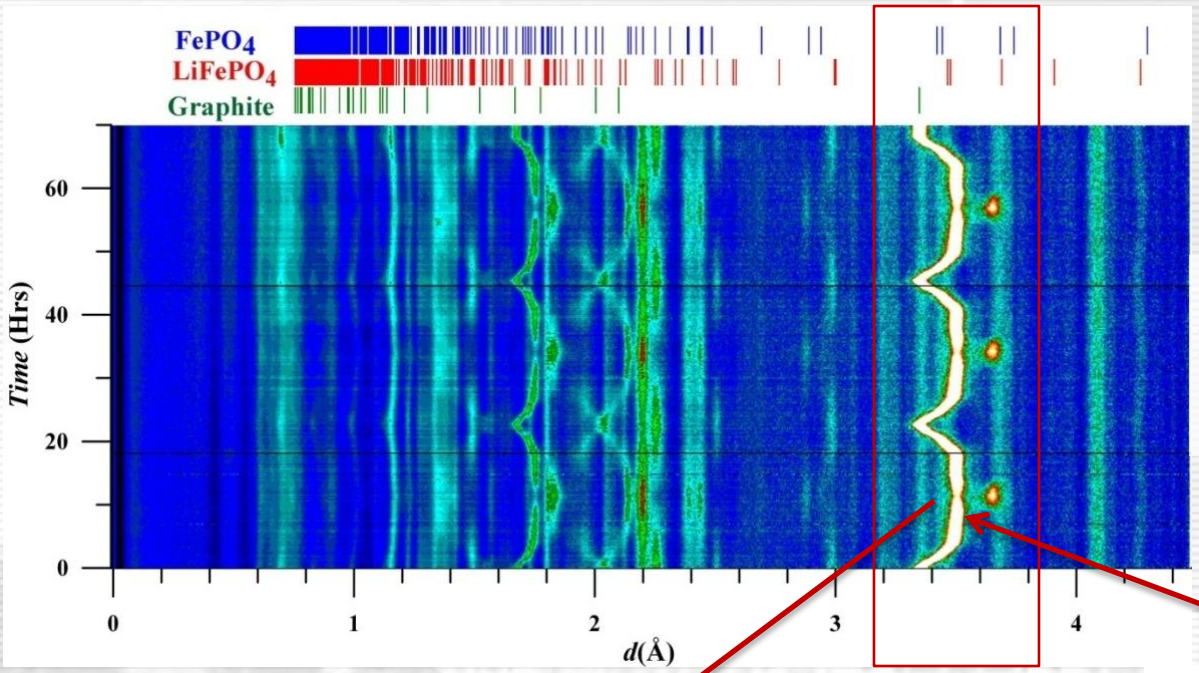

Evolution of the neutron diffraction patterns measured during three charge/discharge (~70 hours) cycles. "Anode window" is marked.

3D view of the "anode-window" region for all three cycles of charge/discharge processes

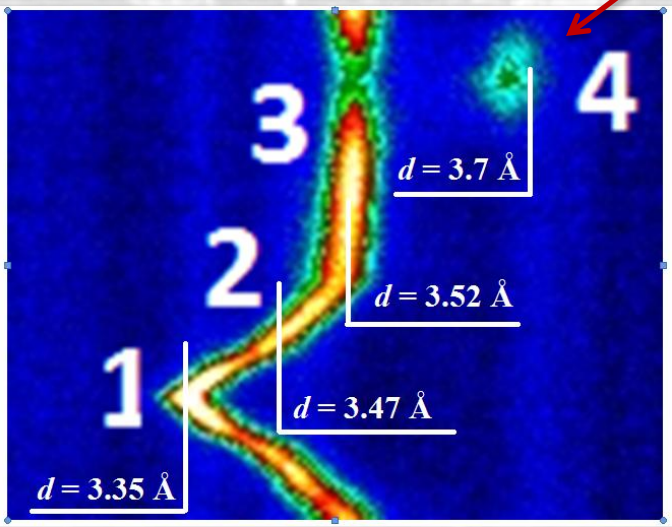

Enlarged chart of the initial (discharged) state with pure graphite line (d = 3.35 Å) and stepwise appearance of LiC_{24} (d = 3.47 Å) and LiC_{12} (d = 3.47 Å).

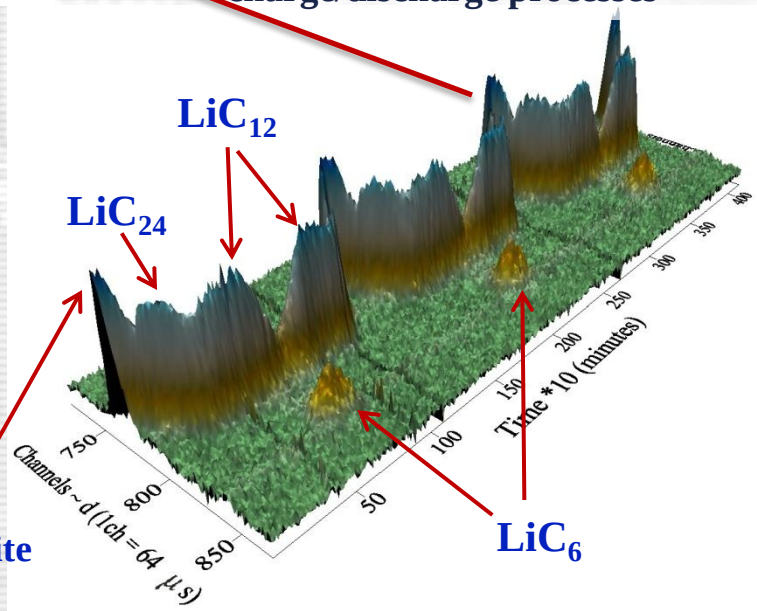

LiC_n phases as seen by neutron diffraction

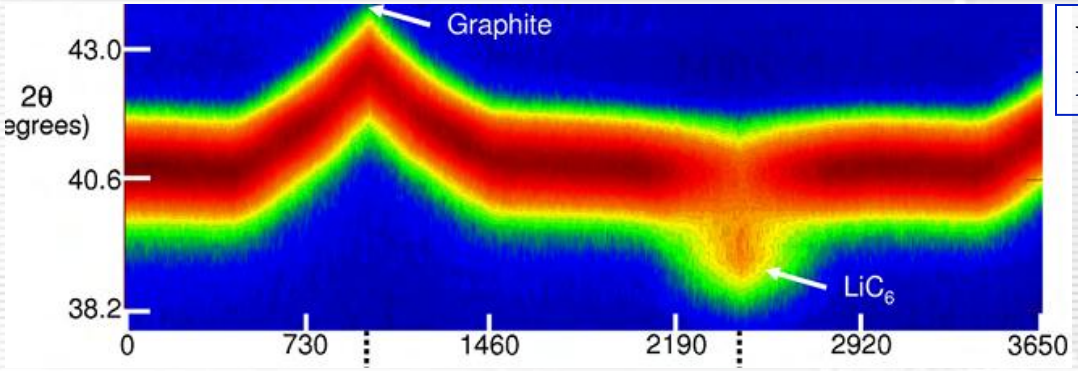

Wombat (ANSTO),
$LiCoO_2 \leftrightarrow LiC_n$

A.Senyshyn et al. (2013)
SPODI (FRM II), λ = 2.54 Å
18650 type cell, $LiCoO_2 \leftrightarrow LiC_n$

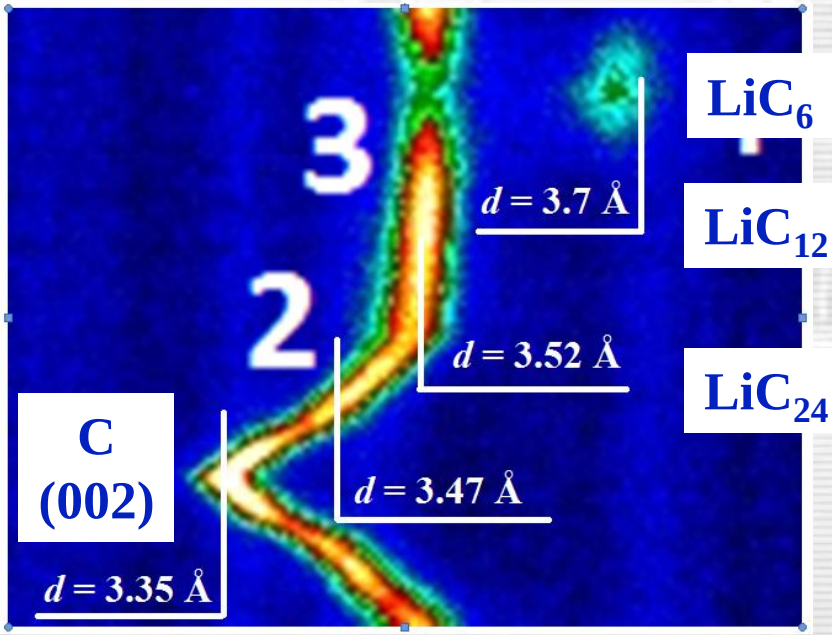

TOF-HRFD (IBR-2), $LiFePO_4 \leftrightarrow LiC_n$

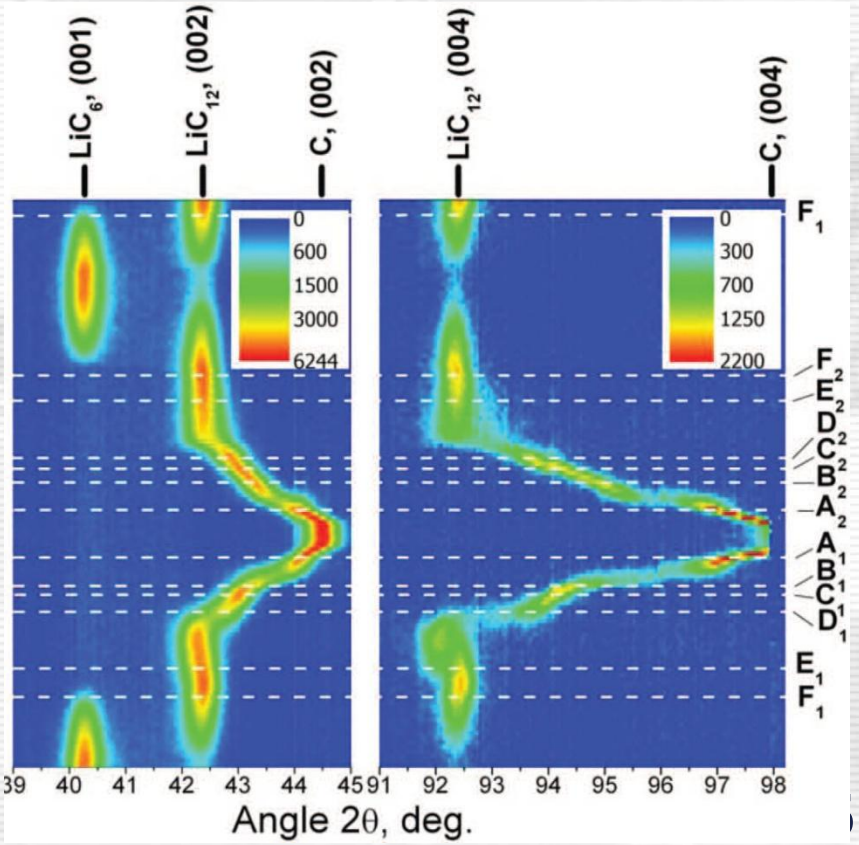

Electrodes: microstructure, defects

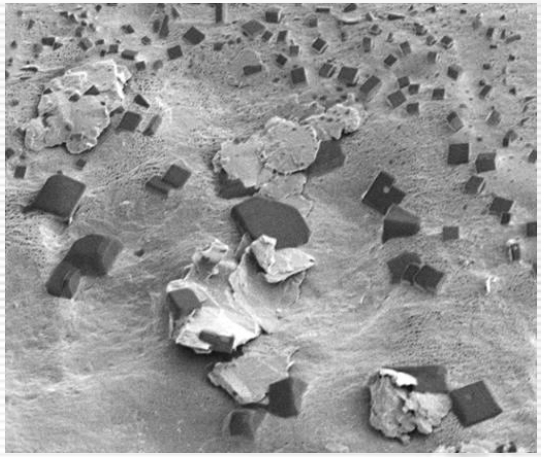

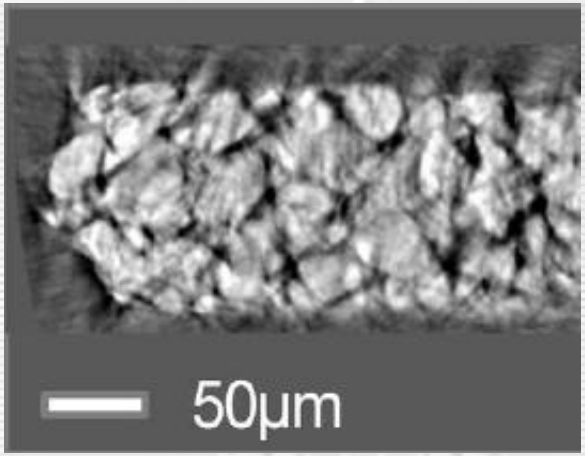

Improvement of conductivity:

- Carbon coating
- Size minimization
- Optimization of morphology

Microstructural analysis

Single line analysis:

- Scherrer
- Stokes – Wilson
- Williamson – Hall
- Warren - Averbach

Top – Down approach:
width and shape parameters

Pattern profile analysis:

WPPF: Rietveld, Pawley

WPPM (Scardi, Leoni)

Bottom - Up approach:
parameters of physical meaning

Microstructure by TOF technique: size and stress effects
(Williamson – Hall plot in *d*-scale)

$$W^2 = C_1 + C_2 d^2 + C_3 d^2 + C_4 d^4$$

Resolution function of TOF-diffractometer

Stress effect, $C_3 \sim \varepsilon^2 \sim (\Delta a/a)^2$

Size effect, $C_4 \sim (1/L)^2$

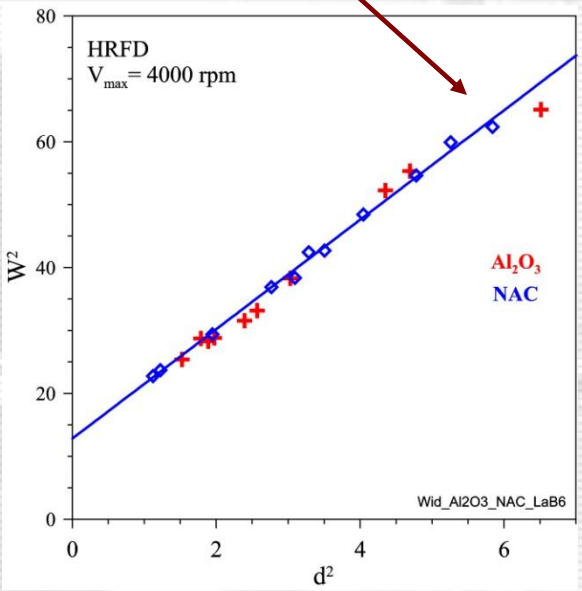

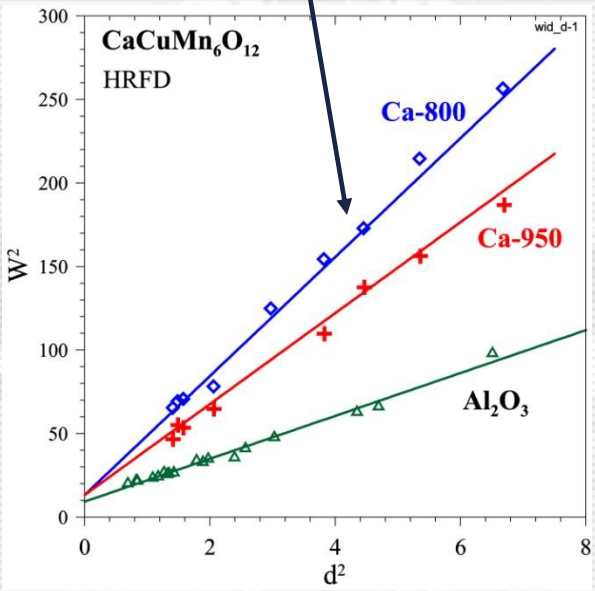

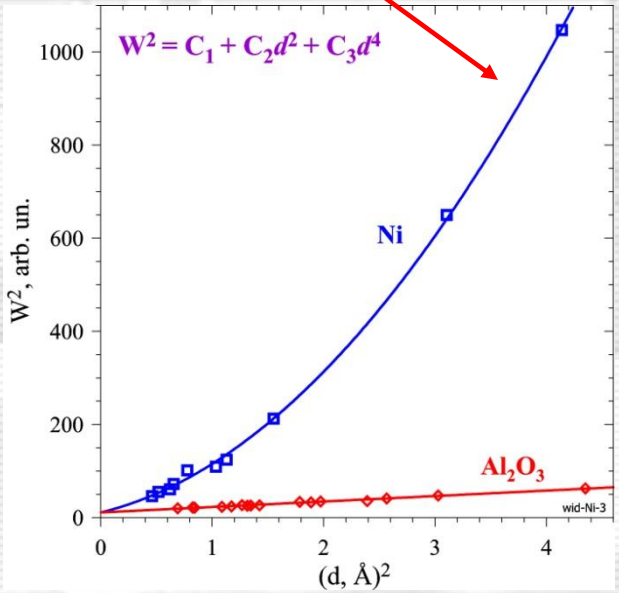

Standard samples (NAC, Al_2O_3) without stresses

Stress effect in $CaCuMn_6O_{12}$

Size effect in nanostructured Ni

Size effects in NiO nanopowders

MSE, 2013

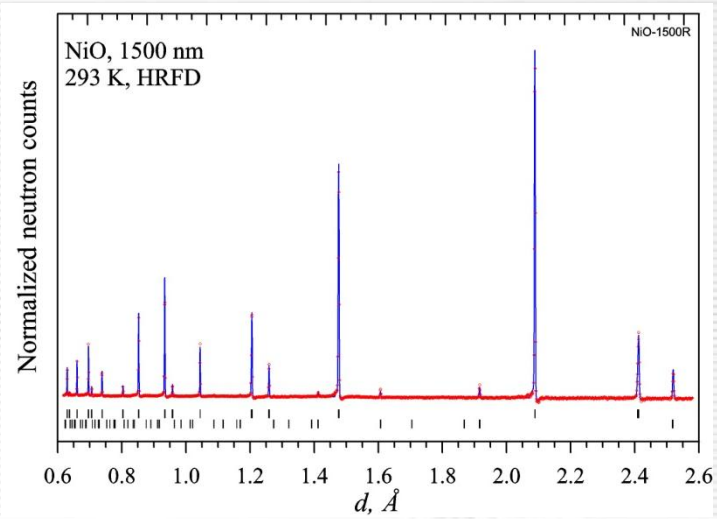

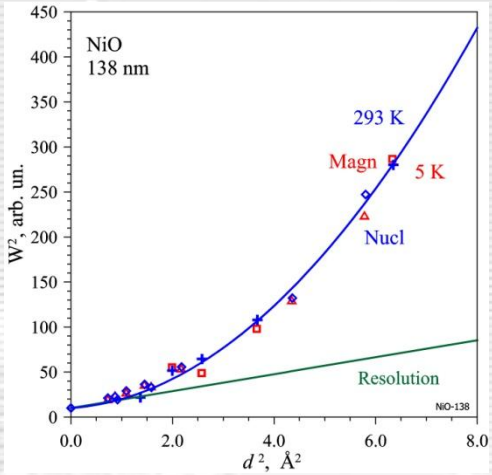

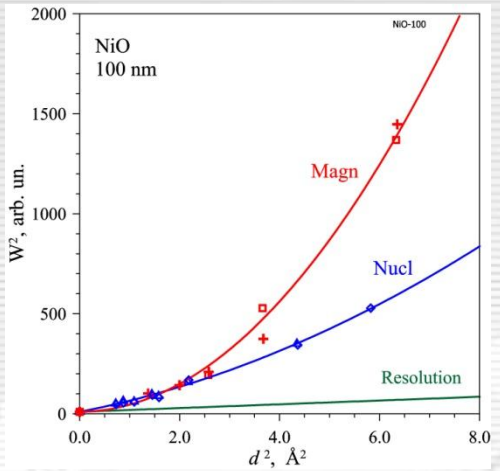

Widths of nuclear and magnetic peaks in diffraction patterns of NiO with 138 nm and 100 nm crystallite size

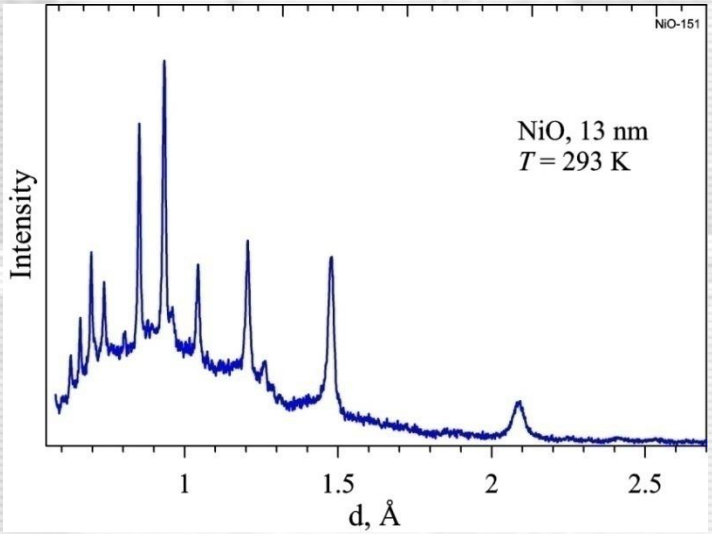

Diffraction patterns of NiO with 13 nm and 138 nm crystallite size

Sample	S4, 1500 nm	S19, 138 nm	S18, 100 nm	S16, 13 nm
L_{nuc}, nm	> 350	102(3)	98(4)	11(2)
L_{mag}, nm	> 350	102(3)	41(3)	10(2)

$L_{nuc} / L_{mag} \approx 2.5$

Microstructure of nanosized $NbC_{0.9}$ powders milled in 1, 5, 10, 15 hours

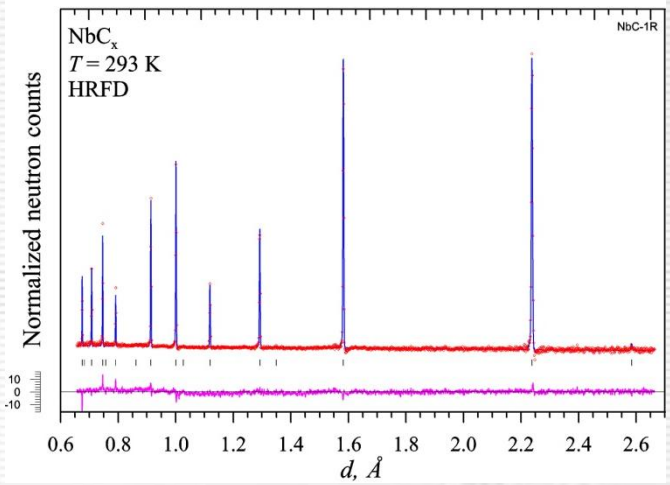

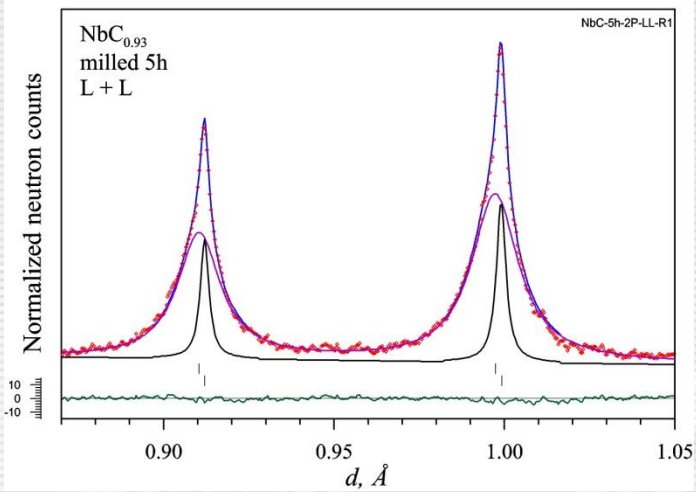

Rietveld refinement of NbC-5h patterns. Positions of components are shifted.

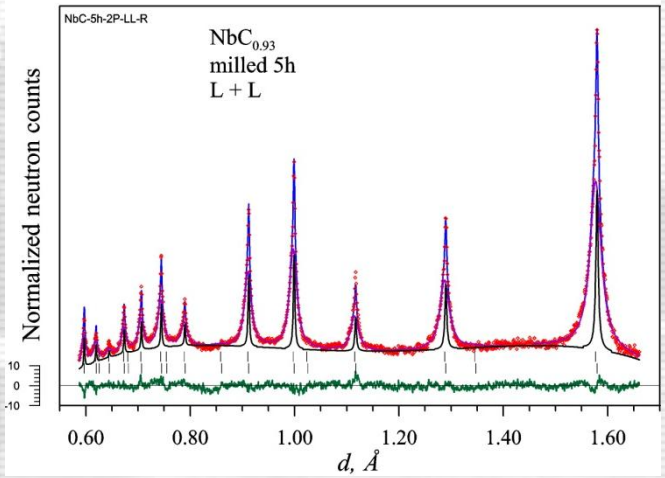

Rietveld refinement of NbC-0h & NbC-5h patterns. Two-component model was used for the second pattern.

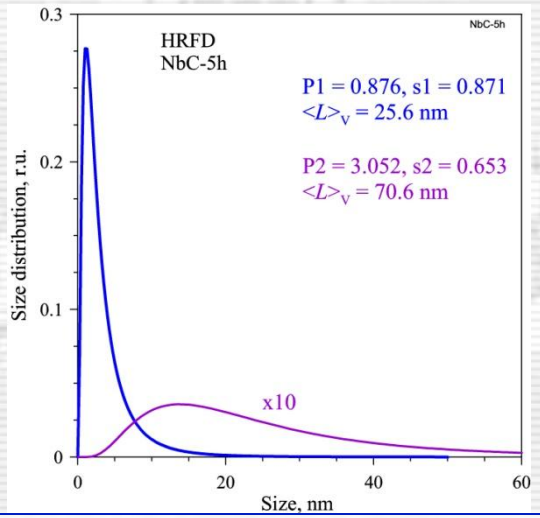

Size distributions for 2 components of NbC-5h. Average sizes are 25.6 and 70.6 nm.

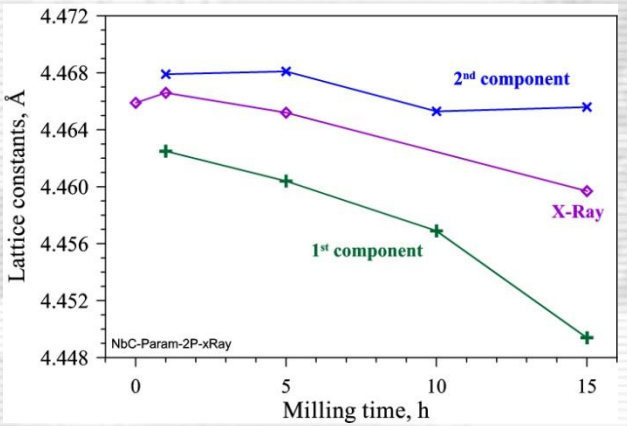

Lattice parameter as a function of milling time for x-ray data and 2 component neutron distribution.

Ex Situ data

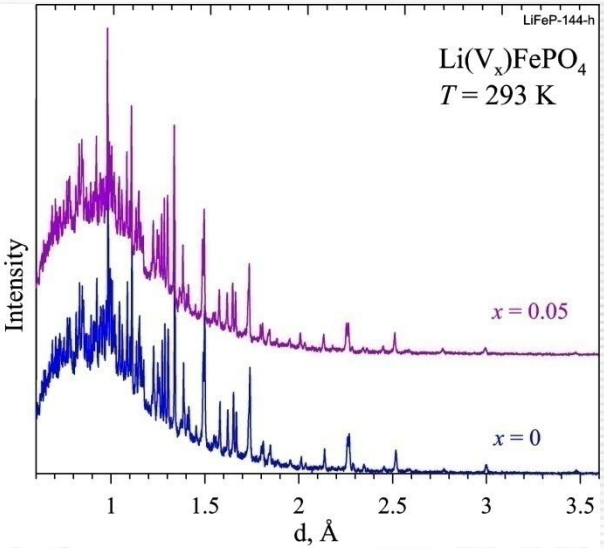

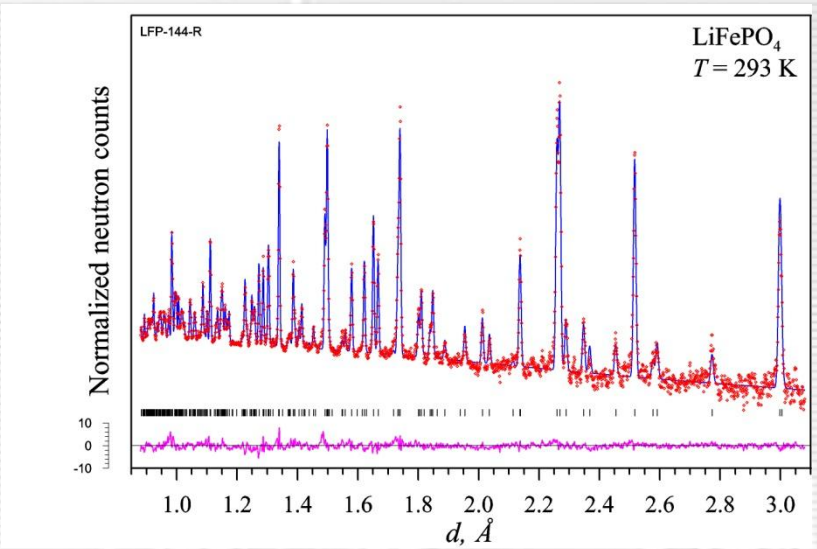

The Rietveld refinement of $LiFePO_4$ diffraction pattern. Coincidence between experiment and calculation is fine.

Raw diffraction patterns of $LiFePO_4$ & $LiFePO_4$:5%V

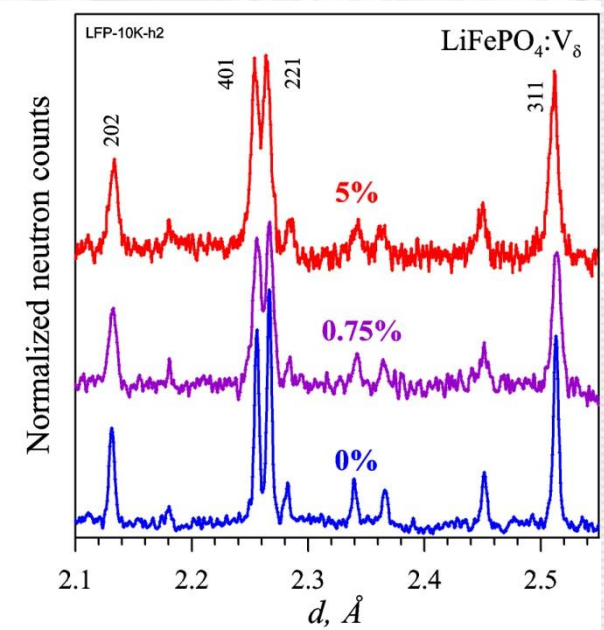

Comparison of diffraction patterns of $LiFePO_4$:V_δ. The width of diffraction lines grows up with δ.

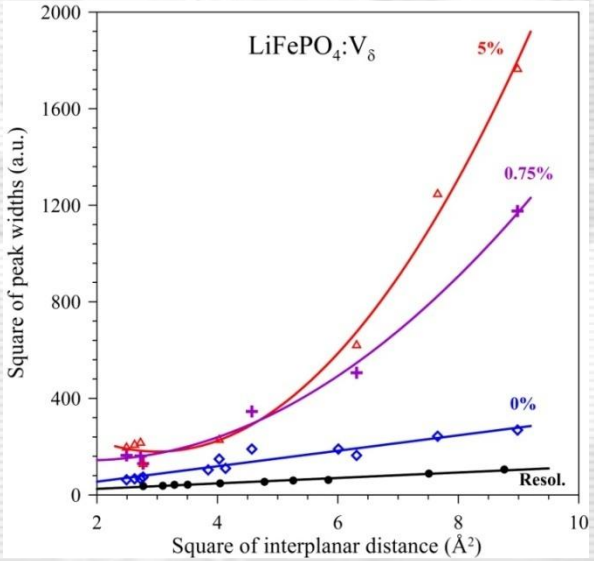

Size effect is clearly seen for $LiFePO_4$ with 0.75%V (L ~ 600 Å) and 5%V (L ~ 400 Å)

In situ neutron reflectometry experiment

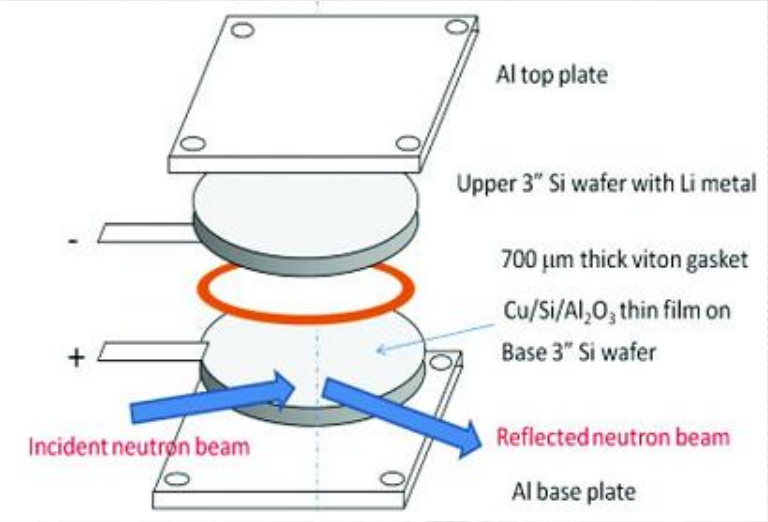

Battery assembly for *in situ* NR

A half cell of electron-beam evaporated Cu (5nm)/Si (10nm)/Al_2O_3 (2nm) films on a Si substrate as the active electrode, Li metal as the counter and negative electrode, and 1 mol/L $LiPF_6$ in EC:DMC (1:1 by volume) solution as the electrolyte.

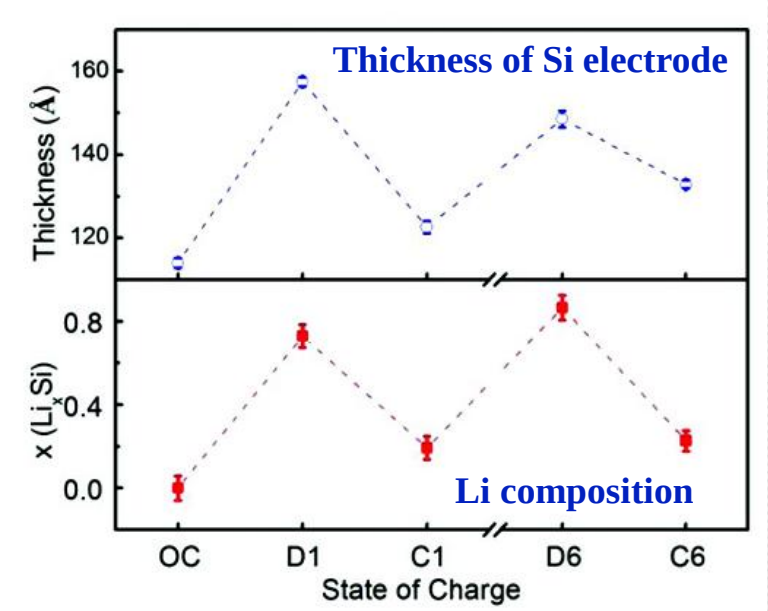

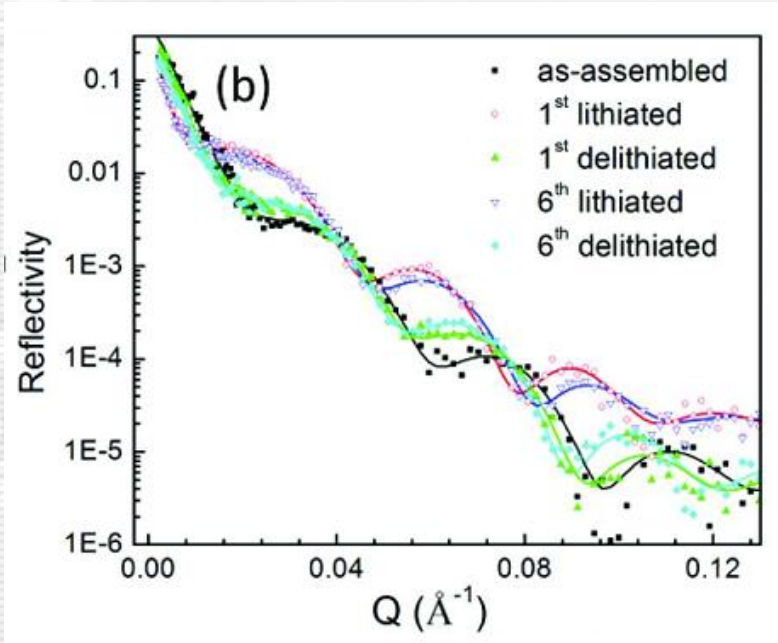

NR spectra at various charge states

from H. Wang et al. "In Situ Neutron Techniques for Studying Lithium Ion Batteries"

In situ small angle neutron scattering (SANS) experiment

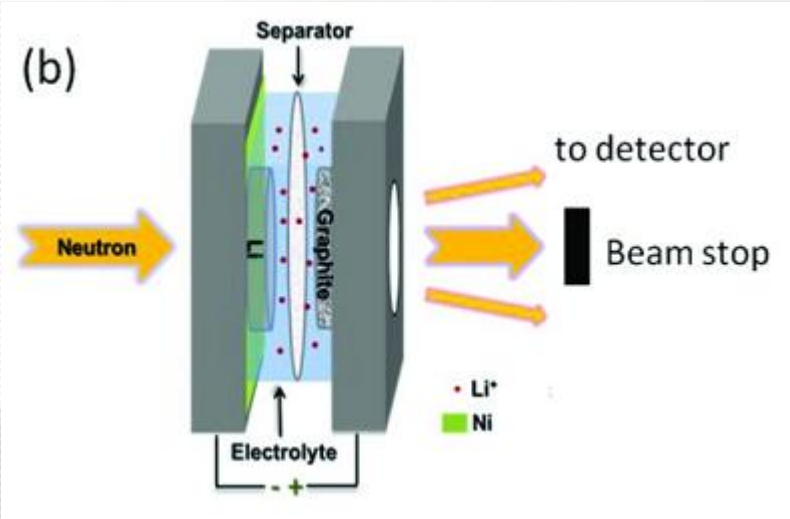

Battery assembly for *in situ* SANS

The variation of integrated SANS intensity upon cyclic charge / discharge is due to the contrast variation induced by lithiation/ delithiation. The excess scattering at higher cycling rates could result from new surfaces created due to fracturing of graphite particles.

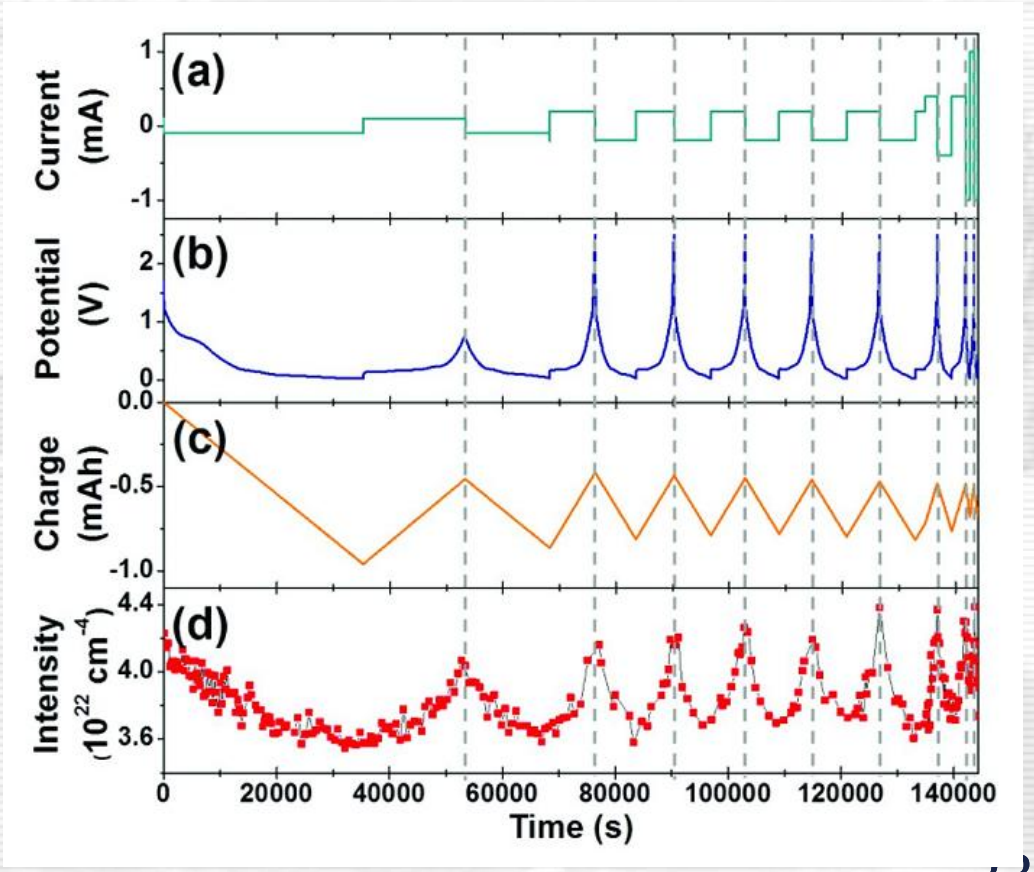

The evolution of:
(a) current,
(b) potential,
(c) charge displacement,
(d) integrated SANS intensity
during charge / discharge cycles

from H. Wang et al. "In Situ Neutron Techniques for Studying Lithium Ion Batteries"

Main components of neutron imaging beam line

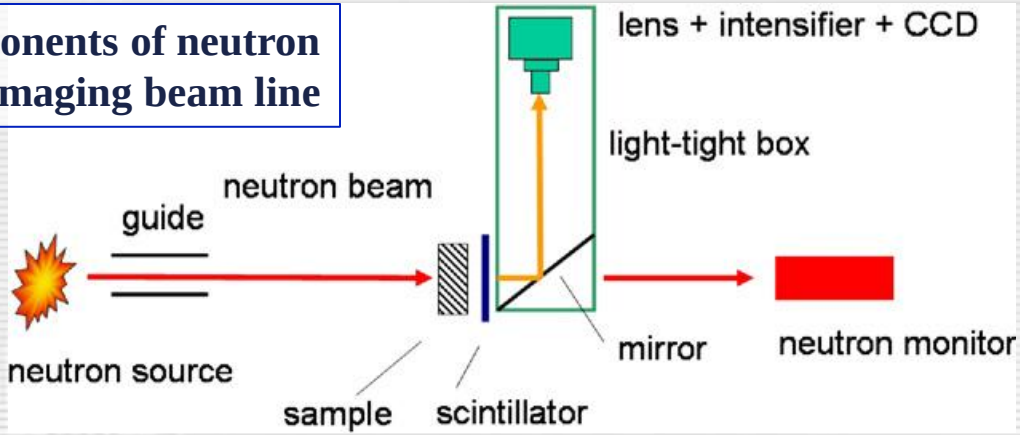

In Situ neutron imaging of alkaline AA cell

(Daniel S. Hussey, NIST, USA)

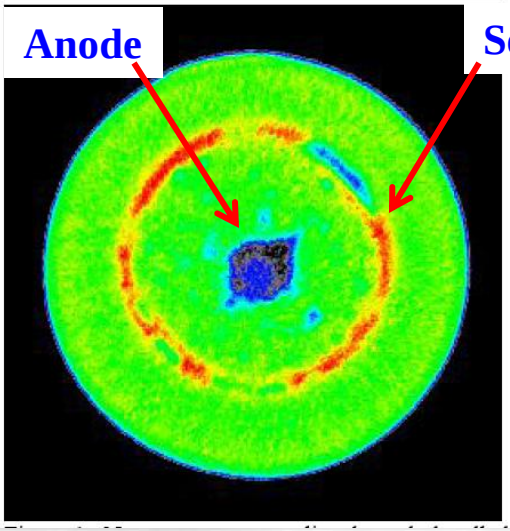

Neutron tomogram slice through the cell before discharge. The anode center post has very low neutron attenuation, while the separator (with hydrogen) has a strong attenuation.

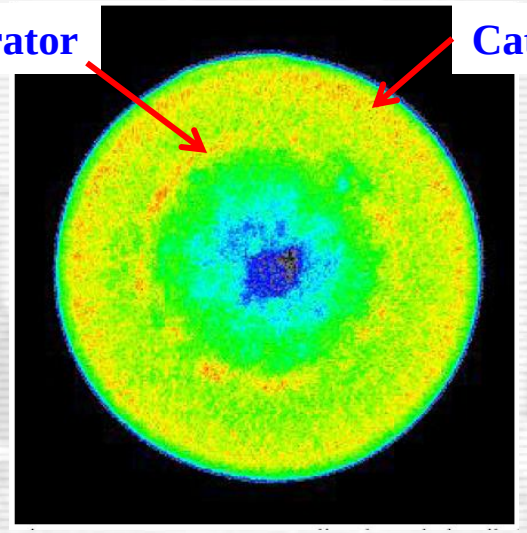

After 17.5 h discharge at a constant current draw of 50 mA. There is increased attenuation in the cathode, indicating migration of hydrogen. The separator is still visible, although it is losing hydrogen.

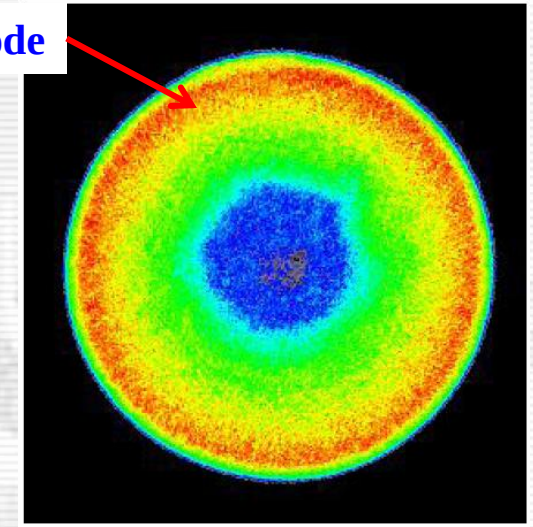

After 52.5 h discharge at a constant current draw of 50 mA. There is further increased attenuation in the cathode. The separator is no longer well defined.

Neutron spectrometers on the IBR-2 reactor

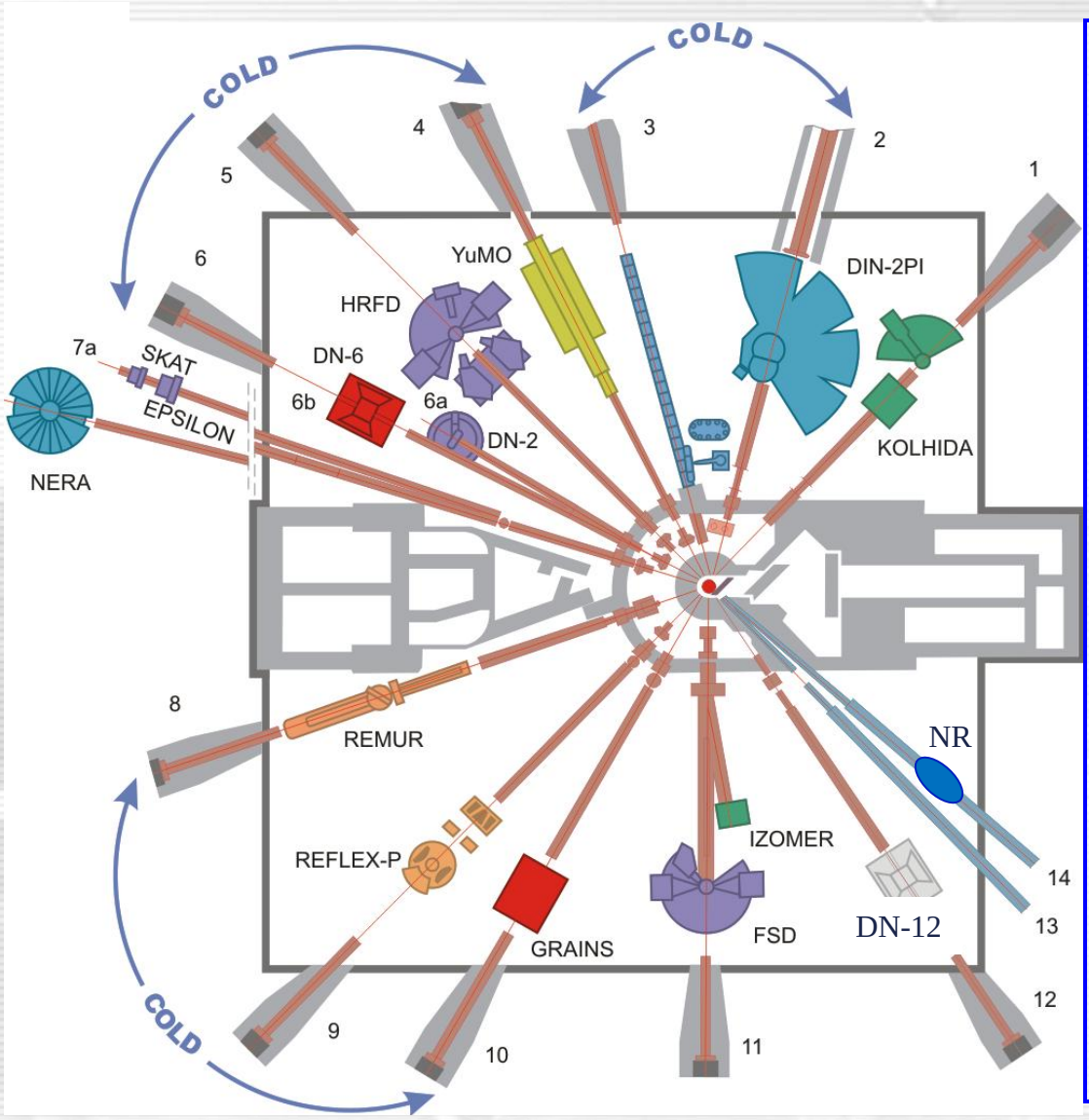

Diffraction (7):

HRFD, SKAT, EPSILON, FSD, DN-12, DN-6, RTD, (FSS)

SANS (1):

YuMO, (SANS-C)

Polarized neutron reflectometry (3):

REMUR, REFLEX, GRAINS

Inelastic scattering (2):

NERA, DIN

Neutron imaging (1):

NR

ИБР-2: дальнейшие планы

1. **“*Real time - in situ* нейтронный структурный анализ материалов и процессов в малогабаритных источниках электрического тока”**

   (Проект РНФ, 2014 – 2016)

   - **$^{7}LiMPO_4$, M = Fe, Mn, Co, Ni и твердые растворы на их основе**
   - **$Na^{7}LiFePO_4F$, $^{7}Li_2CoPO_4F$, $^{7}Li_2FePO_4F$**
   - **оптимизация электрохимических ячеек**

2. **“Нейтронные и рентгеновские (синхротронные) комплементарные исследования реальной структуры кристаллических материалов”**

   (Проект РФФИ-офи_м, 2014 – 2016)

   - **WPPM метод, PM2K software – развитие и адаптация к TOF-данным**
   - **процессы деградации электродных материалов**

3. **“Synchrotron and Neutron Studies for Energy Storage”**

   (Проект ФЦП, 2014 – 2017)

   - **МУРН, рефлектометрия, дифракция**
   - **радиография / томография**

4. **Квазиупругое рассеяние – коэффициенты диффузии???**

You are invited for experiments at the IBR-2 reactor in Dubna – a nice place at the Volga River

In Situ data for commercial battery of 18650 type

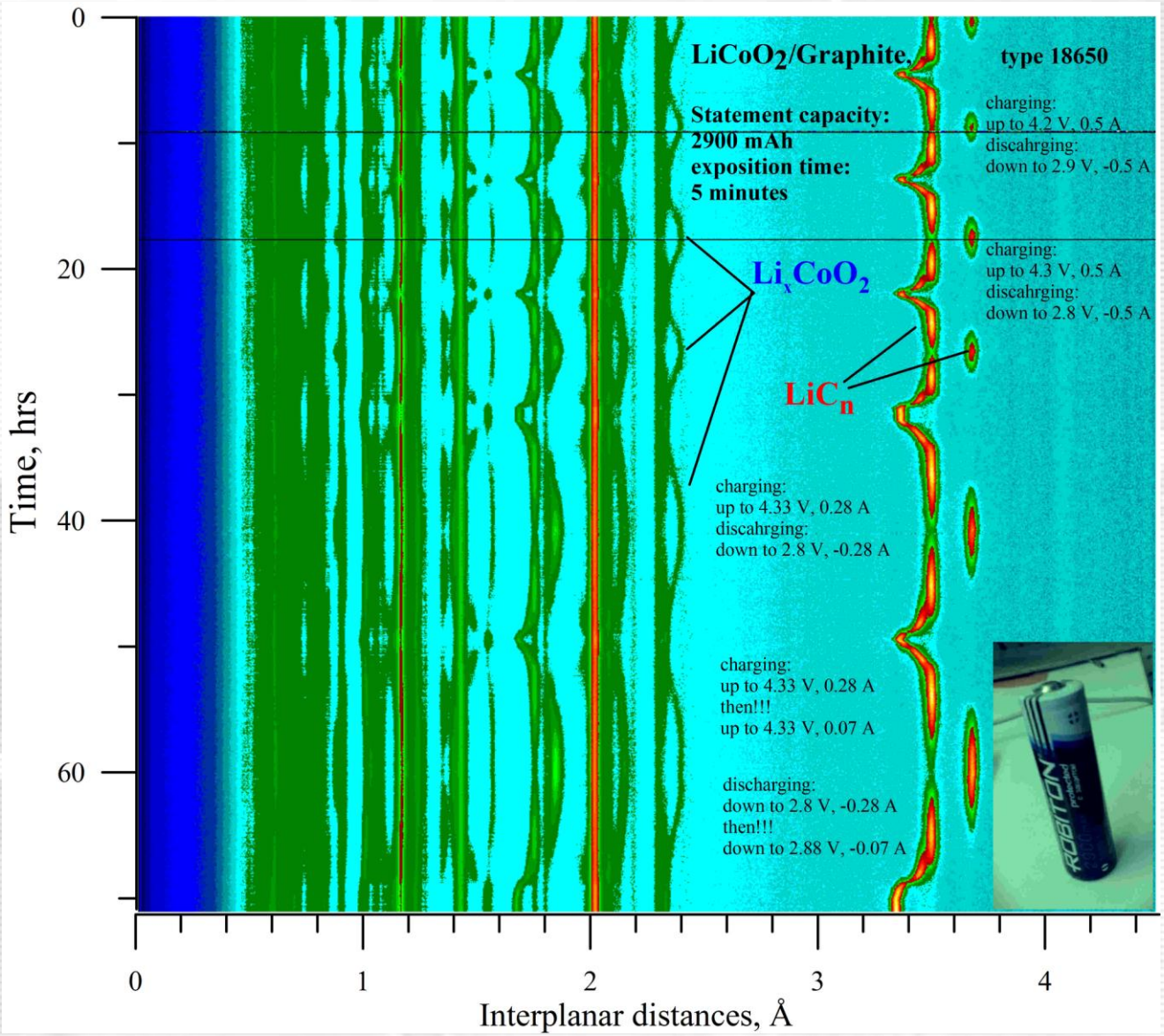

$LiCoO_2$/Graphite based battery of 18650 type.

Statement capacity is 2900 mAh.

Exposition time is 5 min.

Analysis of various charge/discharge rates.